The Comparison of Rapidly Quenched Co-Sn-B and Fe-Sn-B Alloys

Irena Janotová[1(✉)], Peter Švec Sr.[1], Peter Švec[1], Igor Mako[1],
Dušan Janičkovič[1], Juraj Zigo[1], Jozef Marcin[2], and Ivan Škorvánek[2]

[1] Institute of Physics, Slovak Academy of Sciences, Bratislava, Slovakia
`irena.janotova@savba.sk`
[2] Institute of Experimental Physics, Slovak Academy of Sciences,
Košice, Slovakia

Abstract. The ferromagnetic systems based on Fe-Sn-B, Co-Sn-B and Fe-Co-Sn-B were studied in nanocrystalline state due to their interesting magnetic properties that are caused by the homogeneous and ultrafine structure. The alloying of Co-B and/or Fe-B by Sn 3.5 and/or 5 at. % improves the properties of resulting structure composed of the ferromagnetic grains in the amorphous matrix as proved by the XRD and TEM methods. The structure transformation from amorphous to (nano)crystalline state was investigated by DSC and TGA methods and the resulting phase and morphology of crystalline products were analyzed.

Keywords: Soft magnetic materials · Nanocrystalline structure · Iron-boron alloys

1 Introduction

The metastable Fe-B, Co-B and Fe-Co-B alloys are frequently studied and commonly used as a base for different soft magnetic metallic glasses [1–8]. To improve the nanocrystallization of these systems the rare-earth elements are often used. To eliminate the need of these expensive and strategic elements the alloying by the post-transition metals could offer "the fail-back". So that the addition of small amounts of Sn into the Fe-B, Co-B and Fe-Co-B based metastable systems [5–11] was studied. The difference of the atomic radii of Fe and/or Co and Sn atoms are favorable for the incorporation of Sn into the ferromagnetic-rich amorphous phase in spite of a rather low melting point of Sn as compared to Fe or Co ones. Furthermore, Sn is an abundant and inexpensive alloying element [4, 5, 12–15]. In this study the results of the structural and thermodynamic investigation of rapidly quenched $(Fe/Co)_{(85-x)}Sn_xB_{15}$ systems, for the ratio Fe/Co = 1/0, 0/1 and 1/1 and for Sn x = 3.5, 5 at. %.are presented. The structure evolution from amorphous state into the crystalline one was observed by the calorimetric (DSC) and thermogravimetric (TGA) measurements. The formation of ferromagnetic grains from the amorphous matrix is shown by the direct structure observation using transmission electron microscopy as well as by the X-ray diffraction methods. The results of in-situ phase analysis at a pre-defined temperature regime are reviewed, too.

2   Experimental Procedure

The amorphous alloys under investigation were prepared in the form of ribbons 6 mm wide and ~ 20 µm thick by the planar flow casting method. The samples were linearly heated with 10 K/min heating rate and also isothermally annealed at several selected temperatures. The sequence and products of crystallization stages of the amorphous structure at given time and temperature were thus observed. The measurements of temperature dependencies of normalized heat flow and magnetic weight was used to obtain the basic information about the transformation behavior of the studied metallic systems. These methods enable us to define the beginning of the crystallization (temperature of onset of transformation) T_x and to observe the character of the transformations, too. The kinetic parameters (T_x(10 K/min), T_c(10 K/min)) were investigated by differential scanning calorimetry (DSC7 Perkin Elmer) and by thermogravimetry with small applied magnetic field (TGA7 Perkin Elmer), both in the protective argon atmosphere. X-ray diffraction (XRD) using Bruker D8 diffractometer and transmission electron microscopy (TEM) using JEOL 2000FX were used for microstructural characterization of as-cast and isothermally annealed samples. The parameters for the heat-treatment ($T_x - 20$ K for 30 min) were selected according to the resistivity measurements. Magnetic hysteresis loop was acquired using a Forster type B-H loop tracer based on flux-gate magnetometer.

3   Results and Discussion

The rapidly quenched systems usually exhibit typical two-stage transformation from amorphous to nanocrystalline state. The additions of small amounts of alloying element can change this process dramatically. For the systems under investigation it can be seen as the exothermic reactions on the normalized heat flow (Fig. 1a): the two major falls of the heat flow values indicate the two different system structure changes separated in the temperature. Figures 1a and 1b show samples with different Fe/Sn, Fe-Co/Sn and Co/Sn ratio for the constant B. The onset of transformation in the samples containing Fe is shifted towards lower temperature in comparison with the Co based samples. The reduction of the temperature interval between both transformations onsets $-\Delta T$ (Fig. 1a) for the Fe-based samples decrease/disappear with the increasing Co content in the Fe-Co-Sn-B samples. The onsets of the crystallizations stages for the Fe-based samples depend only weakly on the Sn content. For the Co-based samples Sn content is more significant, the transformation pattern is obviously changed into the one step – "polymorphous" crystallization, and for higher -5 at. % Sn content to tree-step transformation; also the shift of T_x to the higher temperatures is seen. For the Fe-Co base sample (in the Fe/Co = 1/1 ratio) the heat flow curve shows two steps of crystallization desirably separated in the time and temperature, while the crystallization temperature T_x is higher than 690 K. The TGA measurements (Fig. 1b) show the Curie temperature of amorphous samples, for Fe based samples in the range of 630 K and 668 K, whereas higher content of Sn affects also higher T_c. Co based samples indicated T_c above the first crystallization stage, but the magnetic weight curves show the decreasing of weight caused by changes in magnetic properties at higher temperatures
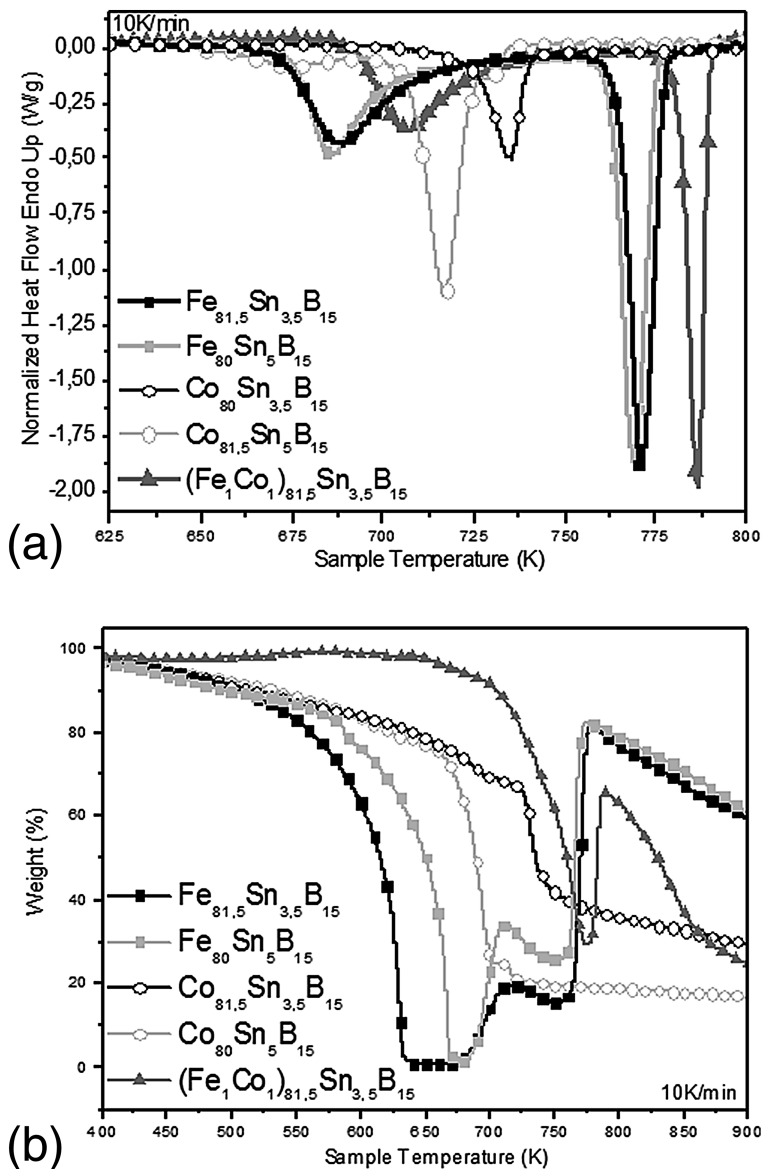
Fig. 1. Temperature dependence of: (a) the normalized heat flow from DSC measurement for the systems with different Fe/Co ratio; (b) the magnetic weight for systems with different Sn content and with different Fe/Co ratio

above 670 K; however, formation of ferromagnetic phase in this temperature region prevents accurate determination of T_c of the amorphous phase. The temperature for isothermal annealing was chosen according to the results of the thermal analysis, with respect to the expected final structure after regulated heat treatment.
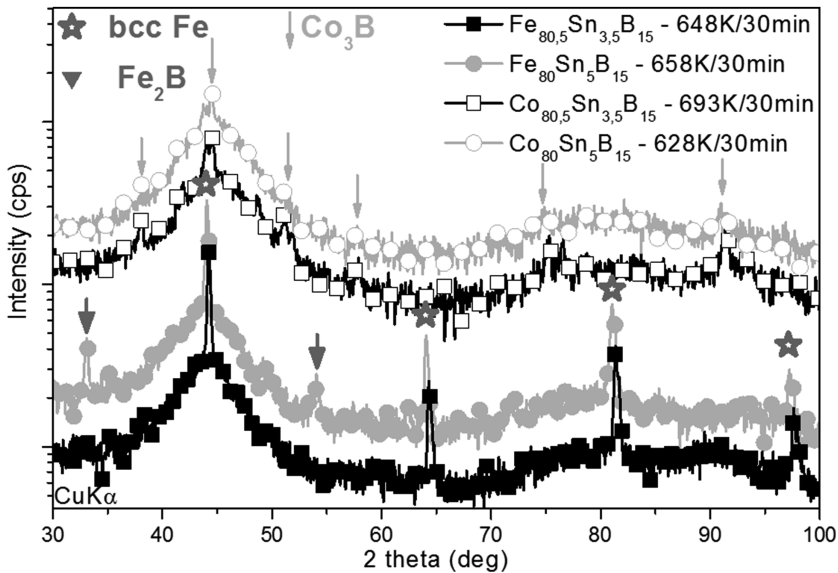
Fig. 2. XRD patterns from Fe-B and Co-B based samples with Sn 3.5 and 5 at. % content after isothermal annealing at temperatures near to T_x for 30 min

The structure of the ferromagnetic phase formed was investigated thoroughly. The XRD analysis of the early stages of the metal rich phase formation from the amorphous state for the samples based on Fe or Co isothermally annealed at temperatures 20 K below T_x was performed. Figure 2 shows the evolution of the metal-rich bcc-Fe and Co_3B phases from the amorphous state in the first crystallization stage. The formation of metalloid-rich phases from the remaining amorphous matrix takes place in the second stage (Fig. 1a). The XRD pattern (Fig. 2) indicates the crystalline bcc-Fe formation for the heat treated Fe-Sn-B samples. The difference in ΔT is visible here, followed by the Fe_2B formation for sample with higher Sn content, as well. Co based samples exhibit one for 3.5 at. % Sn, and three crystallization stages for 5 at. % Sn. The failure of ΔT for these compositions causes an unstable structure and high content of borides created, both responsible for deterioration of magnetic properties. In this perspective, the Fe-Co-Sn-B system appears to be a suitable combination of thermal parameters like T_x, T_c and ΔT (Fig. 1a and b). The structure of $(Fe_1Co_1)_{81.5}Sn_{3.5}B_{15}$ after the isothermal annealing in different stage of structure formation is shown in Fig. 3. The formation of the bcc-Fe phase is shown in Fig. 3a. The measurement of XRD at in situ annealing reveals the ferromagnetic phase evolution from amorphous phase during linear annealing at 2 K/min (Fig. 3b).

Structure after annealing at the temperature of the end of the first transformation (723 K/30 min) exhibits the presence phase in matrix (Fig. 3a), similarly to the Fe-based samples (Fig. 2). From Fig. 4 it is of the bcc-Fe grains in the amorphous matrix (Fig. 3b). Sample annealed at the temperature in the first half of the second transformation (783 K/30 min) exhibit $Fe(Co)_2B$ obvious that the structure after
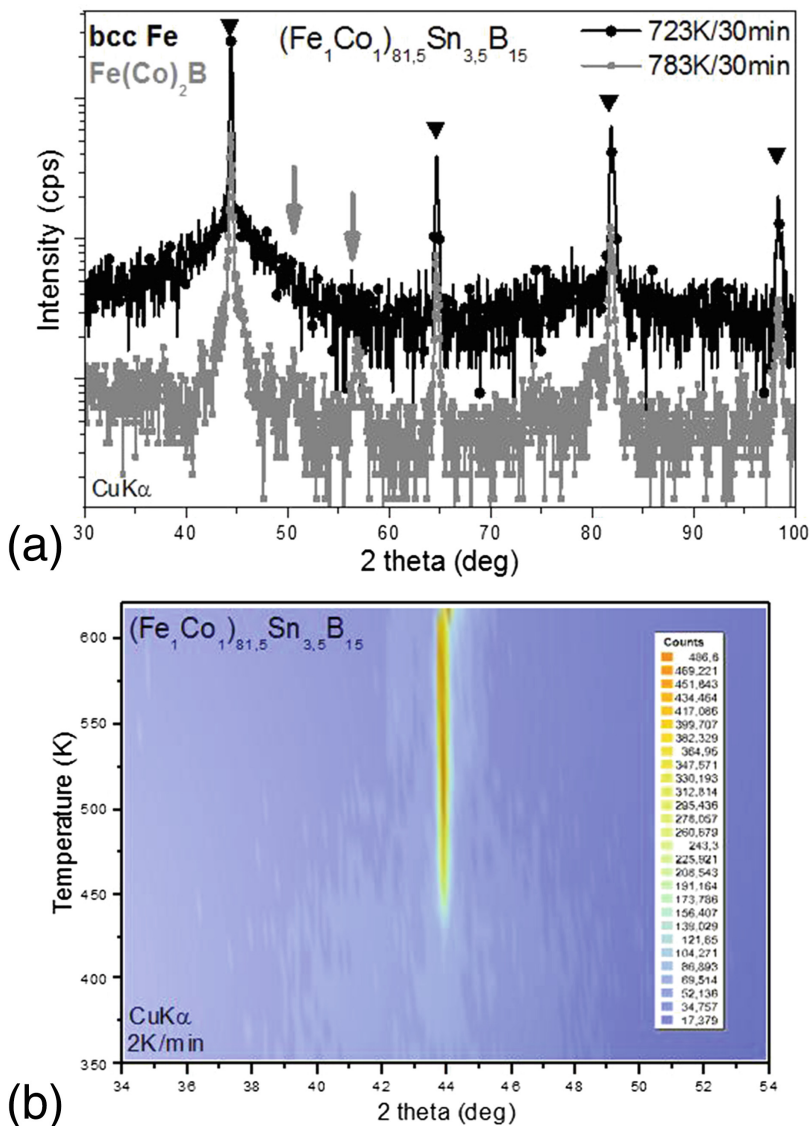
Fig. 3. XRD patterns from Fe-Co-B based samples with Sn 3.5 at. % content: (a) XRD after isothermal annealing at temperatures near to T_x for 30 min; (b) XRD in-situ linear annealing from AQ state

annealing at the temperatures chosen for phase analysis consists of standard small (up to 80 nm) polyhedral bcc-Fe grains for Fe-based samples while more regular Co_2B grains for Co-based samples, surrounded by the amorphous matrix in both cases. TEM images suggest that the difference in ferromagnetic element (Fe or Co) content leads only to a small change in the morphology and crystallinity. For the Fe-Co-based sample
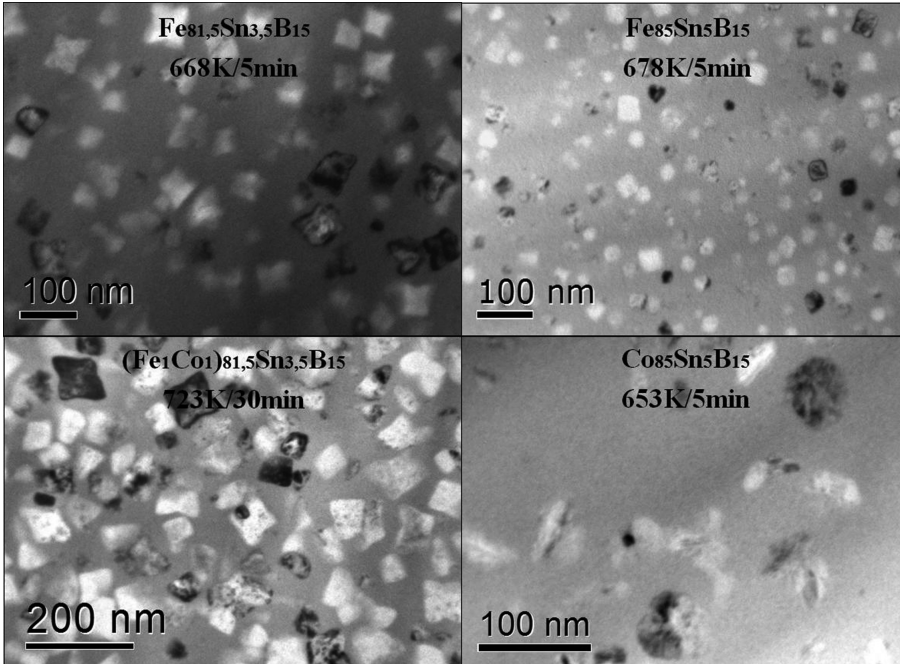
Fig. 4. TEM images showing structure evolution for student compositions after annealing at different temperatures
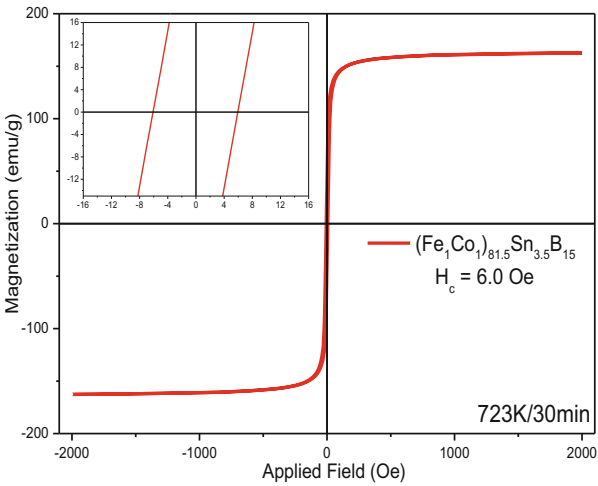

Fig. 5. Quasistatic B-H loop of Fe-Co-Sn-B ribbon annealed at 723 K for 30 min showing the enhanced value of saturation magnetization and coercivity H_c

the grain size and morphology of bcc-Fe(Co) remains unaffected in comparison with the Fe-based samples, but the influence on crystallinity is more obvious. For this sample the observed structure of the ferromagnetic phase could be that one of the expected magnetic properties: the measurement of B-H loop (Fig. 5) exhibits the coercive force H_c = 6 Oe after annealing on 723 K/30 min.

4   Conclusion

Microstructure and compositional dependence of the first transformation stage of Fe-Sn-B, Co-Sn-B and (Fe/Co)-Sn-B based systems were studied. The dependencies of the temperatures of crystallization onsets and of the temperature intervals between the first and next crystallization as well as the position of the Curie temperature relative to the first transformation were investigated. For the Fe-based alloys the crystallization temperature increases with increased Sn content, but this effect is unfavorable for the stability of the resulting ferromagnetic phase. Thus the main interest was focused on the first transformation and the ferromagnetic products n amorphous matrix of (Fe/Co)-Sn-B systems. Diffraction patterns annealed in the vicinity of the first-stage transformation exhibit bcc-Fe (bcc-Fe(Co)) peaks for compositions containing Fe. Materials based on Co only transform into Co_3B containing structures from the beginning – this and the stability of remaining amorphous matrix are not suitable to achieve required magnetic structure. The investigation of combined Fe-Co-Sn-B system with 3.5 at. % of Sn content is more promising. The Fe-Co base has the most suitable influence on the stability of the remaining amorphous phase and its thermal properties, necessary to achieve desirable magnetic properties. The measured B-H loop of (Fe/Co)-Sn-B based system shows high enough saturation magnetization and low values of magnetic coercivity which can be further tuned by proper thermal treatment.

References

1. Herzer, G.: Acta Mater. **61**, 718 (2013)
2. Willard, M.A., Daniil, M.: Handbook of Magnetic Materials, vol. 21, p. 173 (2013)
3. Kemeny, T., et al.: Phys. Rev. B **20**, 476 (1979)
4. Makino, A., et al.: J. Appl. Phys. **91**(10), 8420 (2002)
5. Yoshizawa, Y., et al.: Mater. Sci. Eng. A **375–7**, 207 (2007)
6. Švec, P., et al.: Preparation, processing and selected properties of modern melt-quenched alloys. In: Awrejcewicz, J., Szewczyk, R., Trojnacki, M., Kaliczyńska, M. (eds.) Mechatronics - Ideas for Industrial Application. AISC, vol. 317, pp. 381–396. Springer, Heidelberg (2015). doi:10.1007/978-3-319-10990-9_36
7. Janotova, I., et al.: J. Electr. Eng. **66**, 297–300 (2015)
8. Janotova, I., et al.: J. Alloy. Compd. **615**, 198 (2014)
9. Suzuki, K., et al.: J. Appl. Phys. **70**, 6232 (1991)

10. Ohta, M., Yoshizawa, Y.: J. Magn. Magn. Mater. **320**, 750 (2008)
11. Svec, P., et al.: IEEE Trans. Magn. **46**, 408 (2010)
12. Sharma, P., Zhang, X., Zhang, Y., Makino, A.: Scripta Mater. **95**, 3 (2015)
13. Janotova, I., et al.: J. Supercond. Novel Magn. **26**, 793 (2013)
14. Illekova, E., et al.: J. Alloy. Compd. **509**, S46 (2011)
15. Matko, I., et al.: J. Alloy. Compd. **615**, S462 (2015)